APL Materials

Gliding of conducting dislocations in $SrTiO_3$ at room temperature: Why oxygen vacancies are strongly bound to the cores of dislocations

Cite as: APL Mater. 11, 021108 (2023); https://doi.org/10.1063/5.0126378
Submitted: 15 September 2022 • Accepted: 23 January 2023 • Published Online: 13 February 2023

Christian Rodenbücher, Gustav Bihlmayer, Carsten Korte, et al.

Gliding of conducting dislocations in $SrTiO_3$ at room temperature: Why oxygen vacancies are strongly bound to the cores of dislocations

Cite as: APL Mater. 11, 021108 (2023); doi: 10.1063/5.0126378
Submitted: 15 September 2022 • Accepted: 23 January 2023 •
Published Online: 13 February 2023

Christian Rodenbücher,[1,a)] Gustav Bihlmayer,[2] Carsten Korte,[1] and Kristof Szot[3,4]

AFFILIATIONS

[1] Institute of Energy and Climate Research (IEK-14), Forschungszentrum Jülich GmbH, 52425 Jülich, Germany
[2] Peter Grünberg Institute (PGI-1) and Institute for Advanced Simulation (IAS-1), Forschungszentrum Jülich GmbH and JARA, 52425 Jülich, Germany
[3] aixACCT Systems GmbH, 52068 Aachen, Germany
[4] A. Chełkowski Institute of Physics, University of Silesia, 41-500 Chorzów, Poland

[a)] **Author to whom correspondence should be addressed:** c.rodenbuecher@fz-juelich.de

ABSTRACT

It is well known that the presence of dislocations in solids determines their mechanical properties, such as hardness and plasticity. In the prototype transition metal oxide $SrTiO_3$, dislocations also influence the electronic properties, as they can serve as preferential sites of reduction processes, e.g., supporting the evolution of metallic filaments upon thermal reduction. This indicates that there is a strong interaction between the dislocations and oxygen vacancies formed upon reduction. The latter are locally-compensated by electrons. In order to investigate this interaction, in this study, we analyze the influence of mechanical stress on an already-existing dislocation-based network of conducting filaments in a single crystal. We demonstrate that plastic deformation at room temperature not only modifies the arrangement of dislocations but also conductivity at the nanoscale. This indicates that there is a strong attraction between oxygen vacancies and dislocations, such that the movement of metallic filaments and dislocations under mechanical stress is inseparably coupled.

I. INTRODUCTION

Transition metal oxides with perovskite structures will be key materials in future energy-efficient electronics, as well as sensing and energy conversion.[1–6] Although they have been under scientific investigation for more than six decades, the details of the relationship between crystallographic structure and electronic properties are still not fully understood. Meanwhile, the macroscopic properties of perovskites, such as ionic and electronic conductivity in near-equilibrium conditions, can be described by point defect chemistry in good agreement with experimental results,[7–9] it has been seen that non-equilibrium behavior in the case of very slow matter transport in bulk is far more complex. For instance, a transition between insulating and metallic behavior can be induced by short-time non-equilibrium reduction, resulting in a macroscopic conduction state that is several orders of magnitude higher than the expectation derived from defect chemistry.[10] Evidence from experimental results and theoretical simulations has been gathered indicating that this surprising behavior is related to a non-equilibrium state due to the influence of dislocations that are preferential reduction sites and so can form conducting filaments within the insulating matrix of the crystal.[11] This indicates that oxygen vacancies are located close to the dislocations and thus inducing a local valence change in the transition metal, leading to metallicity.[12]

In this study, we focus on the relationship between oxygen vacancies and structural dislocations and investigate the question of whether vacancies are attracted by the dislocation core. We employ $SrTiO_3$ (STO) as a model material, as it crystallizes in the cubic perovskite structure and is not ferroelectric at room temperature, such that the movement of dislocations is not affected by the presence of domain walls.

II. DISLOCATIONS IN PEROVSKITES

In ionic crystals with an ABO_3 perovskite structure, different types of dislocations can exist. Not only simple edge and screw

dislocations but also partial dislocations are present, which are related to the generation of stacking faults.[13] These partial dislocations can be generated by either a SrO–SrO or a TiO–TiO stacking fault, which results in Sr- and Ti-rich dislocations, respectively.[14] Dislocations in perovskite single crystals are induced in various ways. One source of dislocations is the crystal growth itself, e.g., the frequently used Verneuil method results in bulk dislocation densities of 10^5–10^7 cm^{-2}.[15] Another source of dislocations to be considered is the cutting and polishing process to prepare samples from the crystal boule. This process creates a high dislocation density in the surface layer, which decays exponentially with depth.[16,17] In addition to these fairly unintentional dislocation sources, controlled arrangements of dislocations can be introduced by indentation, scratching, or the preparation of bicrystals.[17–23] It has been found that dislocations can segregate upon irradiation, thermal annealing, or the application of electric fields. Although the position of the sessile dislocations is fixed, the glissile dislocations can move to the crystal lattice by gliding or climbing as long as they do not become pinned.[24,25] The movement of an ensemble of dislocations can result in the formation of complex structures.[26] Dislocations, which are statistically distributed, can undergo polygonization[27] and pile up, which can lead to the evolution of dislocation bundles with a high local dislocation density surrounded by a nearly perfect crystal matrix.[28]

The analysis of the behavior of dislocations under electrical and thermal stress is important for understanding the reduction phenomena. Dislocations are preferential reduction sites and become enriched in oxygen vacancies upon annealing or electro-degradation under reducing conditions.[19,29] As the creation of positively-charged oxygen vacancies is compensated by electrons in the conduction band or localized on cations, reduced dislocations constitute filaments with a high charge carrier concentration embedded in an insulating matrix. As the dislocations are connected to each other due to the invariance of the Burgers vector, a conducting network of filaments evolves. It has been found that in this manner, even a macroscopic filamentary insulator-to-metal transition can be achieved. In this paper, we investigate how such a filamentary network can be further manipulated. We focus on the question of whether the metallic dislocation-based filaments can change their positions with the application of mechanical stress. This raises the question that if the oxygen vacancies are strongly bound to the dislocations, are they tagged along with the moving dislocation? To answer this, we used a simple approach employing plastic deformation at room temperature.[30,31] We create linear agglomerations of dislocations by bending the crystal and subsequently turn these into metallic filaments by means of thermal reduction. Then, we bent the crystal again, this time in an orthogonal direction to the first bending, and analyzed how the conductivity pattern changed.

III. METHODS

Verneuil-grown, epi-polished $SrTiO_3$ single crystals oriented in a (100) orientation (Shinkosha, Yokohama, Japan and CrysTec, Berlin, Germany) were employed in this study. The capacity for deformation was tested by applying mechanical stress by means of an ultrasonic dismembrator.

The bending of the crystals was performed at room temperature by manually pressing them on a rod. The distribution of the dislocations on the surface was made visible by etching the crystals in buffered hydrofluoric acid and analyzing the surface with an optical microscope. A detailed description of the bending procedure and an estimation of the mechanically-induced stress are presented in the supplementary material.

The crystals were reduced under vacuum conditions ($p < 10^{-8}$ mbar) in a quartz tube surrounded by a tube furnace at 900 °C. Local conductivity atomic force microscopy (LC-AFM) was performed using Pt-coated Si tips in contact mode.

Density functional theory (DFT) calculations of defected $SrTiO_3$ were performed using the LDA+U model to describe the localization of the defect states and improve the bandgap.[32] We employed the full potential linearized augmented plane wave method as implemented in the Fleur code (www.flapw.de). All structures were relaxed until the forces were smaller than 50 meV/Å. To further illustrate these relaxations, we calculated "local polarizations" in each unit cell of the chosen supercell based on the distances of Sr and O atoms around the central Ti and their formal charges.

IV. RESULTS AND DISCUSSION

In order to test how easily the STO crystals can be deformed, they were exposed to ultrasonic stress. The morphology of the surface was then analyzed using AFM before and after this procedure, as presented in Fig. 1. It can be seen that the original surface was atomically flat and only terraces with a step height in the range of the lattice constant were present. After the application of mechanical stress, distinct steps with height differences of more than 40 nm oriented along the ⟨100⟩ axes of the crystal evolved. This indicates that this slip system can be easily activated by mechanical stress at room temperature and offers the opportunity to align and agglomerate dislocations in a tailored manner.

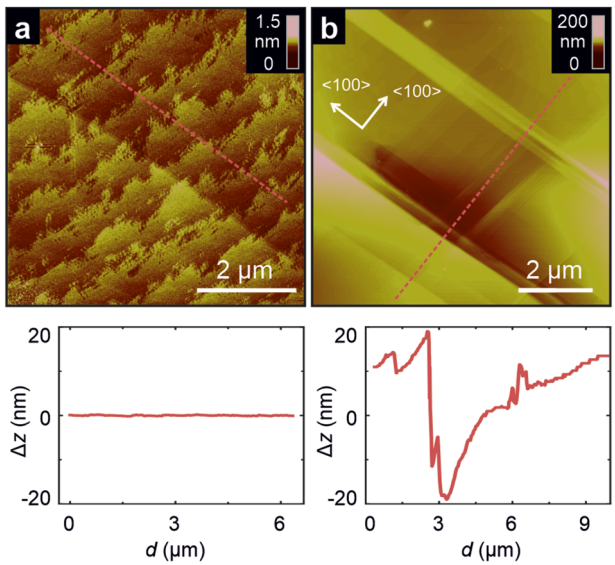

FIG. 1. Surface of the STO crystals (a) before and (b) after applying mechanical stress by an ultrasonic dismembrator mapped by AFM. The bottom figures display profiles extracted along the dotted lines.

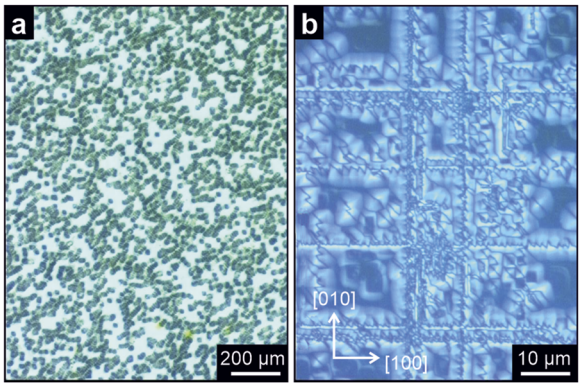

FIG. 2. Etch pits analysis: (a) the pristine polished STO surface; and (b) the surface after bending in two perpendicular ⟨100⟩ directions.

We exploited this effect by bending the crystal in order to induce well-defined dislocation-rich areas. The crystal was first bent in the [100] direction and then thermally-annealed and subsequently bent in the [010] direction after being rotated by 90°. In order to demonstrate that in this manner an ordering of dislocations was induced, etch pit analyses were performed. Figure 2 compares the distribution of the etch pits before and after the bending procedure. It can be seen that the etch pits, which mark the exits of the dislocations, were statistically distributed on the as-received surface. After the bending in two orthogonal ⟨100⟩ directions, a regular arrangement of the etch pits can be identified, proving that a polygonization and redistribution of dislocations were achieved at room temperature.

In the following, we focus on the electrical properties of the dislocations. Figure 3 displays the topography and surface conductivity measured by means of LC–AFM following each preparation step. After the first bending, the evolution of the slip bands resulted

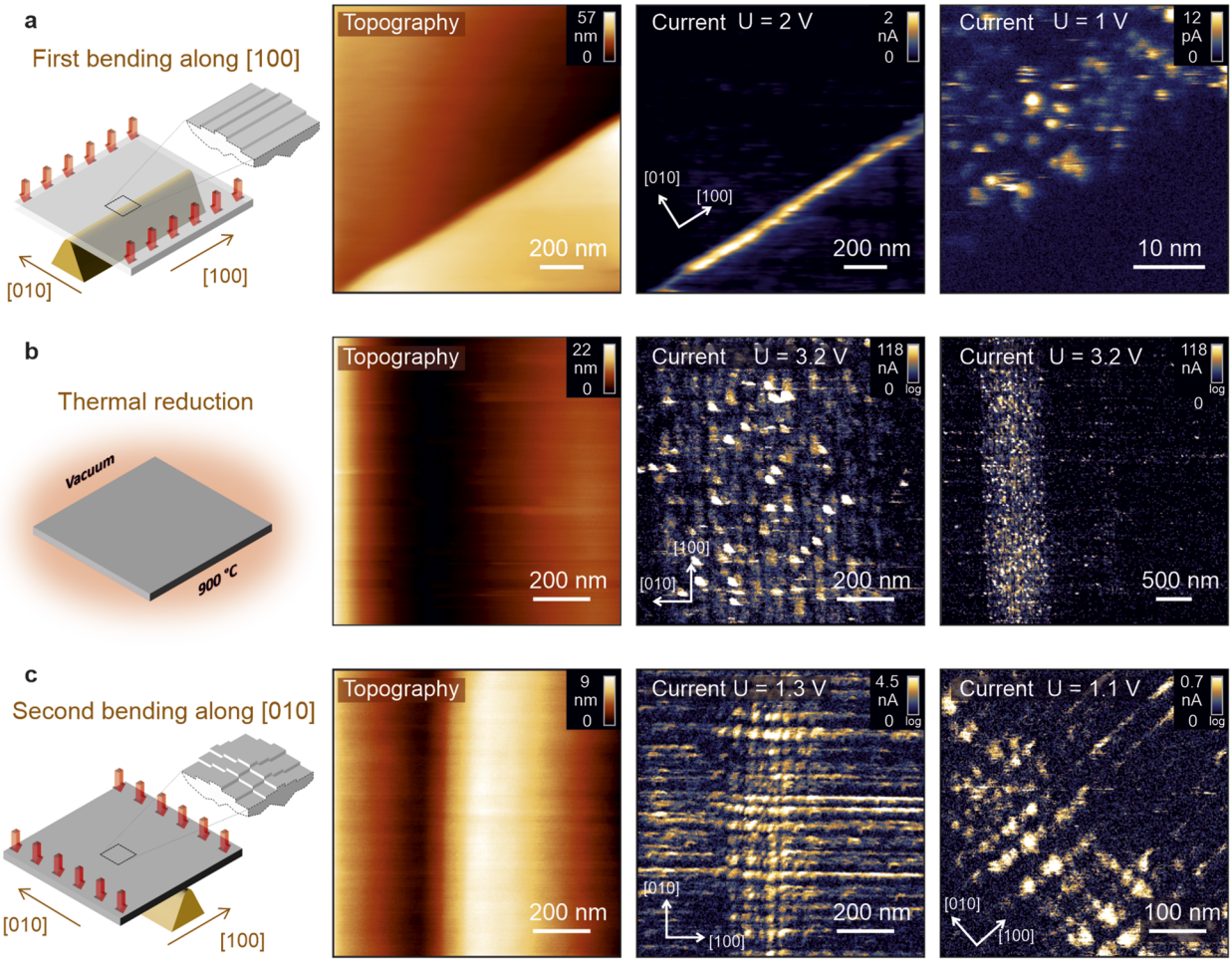

FIG. 3. LC–AFM investigation of the $SrTiO_3$ surface: (a) after the first bending along the [100] direction and slight thermal reduction and activation; (b) after heavy thermal reduction; and (c) after the second bending perpendicular to the first. Note that the scanning direction of (a) and the right panel of (c) were rotated by ~45° with respect to the crystal axes.

in the appearance of distinct steps on the surface. In the example shown in Fig. 3(a), the step had a height of about 50 nm. As the surface did not show any measurable conductivity at room temperature, LC–AFM measurements were performed at elevated temperatures (145–330 °C) under vacuum conditions. This led to a slight reduction and the thermal activation of electronic transport. The corresponding current map reveals that along the step edge, a certain conductivity could be measured, while the conductivity of the remainder of the surface was below the detection limit. A magnified depiction of such a conducting step at a slightly lower temperature illustrates that the conducting areas are arranged in a spot-like structure [see Fig. 3(a), right]. This indicates that the dislocations constitute preferential conduction sites.

Subsequently, the bent crystal was annealed under vacuum conditions at 900 °C. After this process, the conductivity pattern was more pronounced; the alignment of the dislocation-based conducting spots along the slip bands can be clearly identified in Fig. 3(b). Although there were relatively regular arrangements of the conducting spots oriented along the slip band in the [100] direction, the magnitude of the measured current reveals a distinct degree of heterogeneity. There are some spots in which the current is orders of magnitude higher than in others, indicating that in some parts, a bundling of dislocations may occur, resulting in the presence of highly conducting filaments. The overview current map on the right-hand side of Fig. 3(b) reveals that the arrangement of conducting spots follows the dislocation-rich slip band even on a macroscopic scale.

In the final step, the crystal was bent again at room temperature perpendicular to the first bending direction. After this, the conductivity was measured, as shown in Fig. 3(c). The current pattern reveals conducting spots oriented in both bending directions. In order to emphasize that this effect is not induced by the scanning procedure, the sample was turned by 45° with respect to the scanning direction. The resulting image on the right of Fig. 3(c) reveals an alignment of the conducting spots in the ⟨100⟩ direction, proving that this conductivity pattern has, indeed, been induced by the bending procedure. As there was no additional thermal reduction following the second bending procedure, we can conclude that the change in the conductivity pattern relates to the movement of conducting dislocations at room temperature under the applied mechanical stress. As a result, this implies that when a reduced dislocation moves in a stress field, the oxygen vacancies, being responsible for the local valence change in the Ti, which lead to the metallic conductivity, must also move. Hence, there must be an attractive interaction between dislocations and oxygen vacancies. In order to support this assumption, DFT simulations were performed. For the sake of simplicity, we simulated the dislocation as inner surface in the crystal by removing a slab with a width of three unit cells from the (6 × 5 × 1) supercell, as illustrated in Fig. 4. Then, extended oxygen vacancies were created at the positions marked 1–8, with the vacancy formation energy at 8 being considered bulk-like. As can be seen from the lower panel, the vacancy formation energy drops significantly near the dislocation. Some asymmetry can be seen between the upper right and lower left edges of the dislocation, probably relating to the different local environments at the inner surfaces and the local polarization, as indicated by the blue arrows. Of course, not all possible vacancy positions were considered, but from the large energy differences (up to 0.7 eV), a strong interaction between the

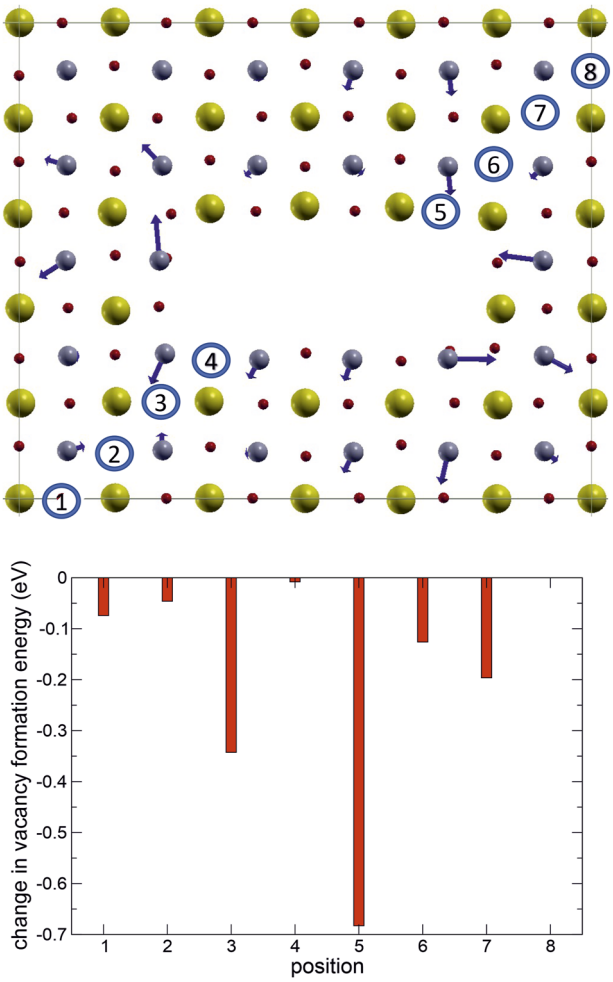

FIG. 4. 6 × 5 unit cell of $SrTiO_3$ with three unit cells in the center removed. Yellow, gray, and red spheres indicate Sr, Ti, and O atoms, respectively. The blue arrows represent the local polarization created around the defect, whereas the blue circles indicate the positions of the extended O defects considered. Bottom: DFT calculations of the change in oxygen vacancy formation energy for the positions marked in the top panel. The reference point is selected at position 8.

defect and inner surfaces can be deduced. Thus, a movement of this inner surface will drag along the extended O defects.

In addition to this simple energetic criterion, there are also further arguments supporting the assumption of an attractive interaction between vacancies and dislocations. Although STO is dielectric at room temperature, the symmetry of the crystal lattice is locally broken close to the dislocations. Hence, the ferroelectric and flexoelectric effects become relevant,[33] as we also previously demonstrated using piezoelectric force microscopy.[34] It has been shown that the dislocation core constitutes a kind of dipole, and its interaction with the positively-charged oxygen vacancies could lead to a synchronous motion of the vacancies with the dislocations.[24,35] This mechanism is supported by the DFT simulations discussed previously, which indicate an attractive interaction between dislocations and vacancies. Furthermore, one could consider mechanical stress

and assume that the sum of the mechanical energies of the ferroelastic dislocation core and the mechanical energy of the individual oxygen vacancies is minimal when the vacancy is located in the dislocation core. Hence, the movement of the dislocations should automatically lead to the joint co-displacement of the deformation of the vacancies.

In summary, we have demonstrated that it is possible to manipulate the surface conductivity of reduced STO via mechanical stress. Metallic filaments, which were formed during thermal reduction along the dislocations, change their position in conjunction with the movement of the dislocations. Supported by *ab initio* simulations, we conclude that there is an attractive interaction between the dislocation core and oxygen vacancies. Hence, a movement of dislocations with TiO_x cores, which constitute metallic filaments, can be induced by means of mechanical stress without breaking their galvanic connection. It also has to be kept in mind that the thermal reduction of STO can lead to the evolution of a variety of Ti-rich suboxides close to the dislocation cores, such as Magnéli phases or more complex structures such as $Sr_2Ti_6O_{13}$ or $Sr_1Ti_{11}O_{20}$, which have been found during filament formation in resistive switching devices.[28,36–38] Investigating how these secondary phases behave under mechanical stress and influence the movement of filaments is a challenging task for future research.

Our finding that dislocation-based conducting filaments can be moved mechanically may be relevant to explain, e.g., the degradation processes of devices under mechanical stress and could also open up opportunities for tailoring the electronic properties of oxide materials by mechanical engineering. Aligning dislocations using mechanical stress might help to realize the idea of Shockley, who postulated back in 1983 that conducting dislocations in semiconductors could hold technological promise as nano-transistors or electrical tweezers.[39]

SUPPLEMENTARY MATERIAL

See the supplementary material for an estimation of the mechanical stress induced by the manual bending method.

ACKNOWLEDGMENTS

We gratefully acknowledge C. Wood for proofreading the manuscript. Open Access publication funded by the Deutsche Forschungsgemeinschaft (DFG, German Research Foundation)—Grant No. 491111487. G.B. gratefully acknowledges computing time granted through JARA-HPC on the supercomputer JURECA at Forschungszentrum Jülich.

AUTHOR DECLARATIONS

Conflict of Interest

The authors have no conflicts to disclose.

Author Contributions

Christian Rodenbücher: Conceptualization (equal); Data curation (equal); Formal analysis (equal); Validation (equal); Visualization (equal); Writing – original draft (equal); Writing – review & editing (equal). **Gustav Bihlmayer**: Conceptualization (equal); Investigation (equal); Validation (equal); Visualization (equal); Writing – review & editing (equal). **Carsten Korte**: Conceptualization (equal); Writing – review & editing (equal). **Kristof Szot**: Conceptualization (equal); Data curation (equal); Formal analysis (equal); Investigation (equal); Validation (equal); Visualization (equal); Writing – review & editing (equal).

DATA AVAILABILITY

The data that support the findings of this study are available from the corresponding author upon reasonable request.

REFERENCES

[1] F. Gunkel, D. V. Christensen, Y. Z. Chen, and N. Pryds, Appl. Phys. Lett. **116**, 120505 (2020).
[2] B. L. Phoon, C. W. Lai, J. C. Juan, P.-L. Show, and W.-H. Chen, Int. J. Energy Res. **43**, 5151 (2019).
[3] B. Szafraniak, Ł. Fuśnik, J. Xu, F. Gao, A. Brudnik, and A. Rydosz, Coatings **11**, 185 (2021).
[4] K. Szot, W. Speier, G. Bihlmayer, and R. Waser, Nat. Mater. **5**, 312 (2006).
[5] J. Hwang, R. R. Rao, L. Giordano, Y. Katayama, Y. Yu, and Y. Shao-Horn, Science **358**, 751 (2017).
[6] R. Waser, R. Dittmann, G. Staikov, and K. Szot, Adv. Mater. **21**, 2632 (2009).
[7] C. Rodenbücher, C. Korte, T. Schmitz-Kempen, S. Bette, and K. Szot, APL Mater. **9**, 011106 (2021).
[8] N. D. Wood, D. M. Teter, J. S. Tse, R. A. Jackson, D. J. Cooke, L. J. Gillie, S. C. Parker, and M. Molinari, J. Solid State Chem. **303**, 122523 (2021).
[9] M. Siebenhofer, F. Baiutti, J. de Dios Sirvent, T. M. Huber, A. Viernstein, S. Smetaczek, C. Herzig, M. O. Liedke, M. Butterling, A. Wagner, E. Hirschmann, A. Limbeck, A. Tarancon, J. Fleig, and M. Kubicek, J. Eur. Ceram. Soc. **42**, 1510 (2022).
[10] C. Rodenbücher, C. Guguschev, C. Korte, S. Bette, and K. Szot, Crystals **11**, 744 (2021).
[11] D. Marrocchelli, L. Sun, and B. Yildiz, J. Am. Chem. Soc. **137**, 4735 (2015).
[12] C. Rodenbücher, K. Bittkau, G. Bihlmayer, D. Wrana, T. Gensch, C. Korte, F. Krok, and K. Szot, Sci. Rep. **10**, 17763 (2020).
[13] K. Szot, C. Rodenbücher, G. Bihlmayer, W. Speier, R. Ishikawa, N. Shibata, and Y. Ikuhara, Crystals **8**, 241 (2018).
[14] L. Porz, T. Frömling, A. Nakamura, N. Li, R. Maruyama, K. Matsunaga, P. Gao, H. Simons, C. Dietz, M. Rohnke, J. Janek, and J. Rödel, ACS Nano **15**, 9355 (2021).
[15] C. Guguschev, Z. Galazka, D. J. Kok, U. Juda, A. Kwasniewski, and R. Uecker, CrystEngComm **17**, 4662 (2015).
[16] L. Jin, X. Guo, and C. L. Jia, Ultramicroscopy **134**, 77 (2013).
[17] C. Rodenbücher, D. Wrana, T. Gensch, F. Krok, C. Korte, and K. Szot, Crystals **10**, 665 (2020).
[18] C. Okafor, K. Ding, X. Zhou, K. Durst, J. Rödel, and X. Fang, J. Am. Ceram. Soc. **105**, 2399 (2022).
[19] C. Rodenbücher, S. Menzel, D. Wrana, T. Gensch, C. Korte, F. Krok, and K. Szot, Sci. Rep. **9**, 2502 (2019).
[20] S. Stich, K. Ding, Q. K. Muhammad, L. Porz, C. Minnert, W. Rheinheimer, K. Durst, J. Rödel, T. Frömling, and X. Fang, J. Am. Ceram. Soc. **105**, 1318 (2022).
[21] F. Javaid, A. Stukowski, and K. Durst, J. Am. Ceram. Soc. **100**, 1134 (2017).
[22] S. Kondo, N. Shibata, T. Mitsuma, E. Tochigi, and Y. Ikuhara, Appl. Phys. Lett. **100**, 181906 (2012).
[23] S. Kondo, T. Mitsuma, N. Shibata, and Y. Ikuhara, Sci. Adv. **2**, e1501926 (2016).
[24] P. Hirel, G. F. B. Moladje, P. Carrez, and P. Cordier, Phys. Chem. Miner. **46**, 37 (2019).
[25] P. Hirel, P. Carrez, and P. Cordier, Scr. Mater. **120**, 67 (2016).
[26] M. D. Armstrong, K.-W. Lan, Y. Guo, and N. H. Perry, ACS Nano **15**, 9211 (2021).
[27] K. C. Le and B. D. Nguyen, Int. J. Eng. Sci. **59**, 211 (2012).

[28]K. Szot, G. Bihlmayer, and W. Speier, in *Solid State Physics*, edited by R. E. Camley and R. L. Stamps (Academic Press, 2014), Vol. 65, pp. 353–559.
[29]L. L. Rusevich, M. Tyunina, E. A. Kotomin, N. Nepomniashchaia, and A. Dejneka, Sci. Rep. **11**, 23341 (2021).
[30]K.-H. Yang, N.-J. Ho, and H.-Y. Lu, J. Am. Ceram. Soc. **94**, 3104 (2011).
[31]P. Gumbsch, S. Taeri-Baghbadrani, D. Brunner, W. Sigle, and M. Rühle, Phys. Rev. Lett. **87**, 085505 (2001).
[32]A. Al-Zubi, G. Bihlmayer, and S. Blügel, Crystals **9**, 580 (2019).
[33]P. Gao, S. Yang, R. Ishikawa, N. Li, B. Feng, A. Kumamoto, N. Shibata, P. Yu, and Y. Ikuhara, Phys. Rev. Lett. **120**, 267601 (2018).
[34]A. Bussmann-Holder, H. Keller, A. Simon, G. Bihlmayer, K. Roleder, and K. Szot, Crystals **10**, 437 (2020).
[35]M. Landeiro Dos Reis, P. Carrez, and P. Cordier, Phys. Rev. Mater. **5**, 063602 (2021).
[36]W. Lee, S. Yoo, K. J. Yoon, I. W. Yeu, H. J. Chang, J.-H. Choi, S. Hoffmann-Eifert, R. Waser, and C. S. Hwang, Sci. Rep. **6**, 20550 (2016).
[37]K. R. Udayakumar and A. N. Cormack, J. Am. Ceram. Soc. **71**, C469 (1988).
[38]M. Fujimoto and M. Watanabe, J. Mater. Sci. **20**, 3683 (1985).
[39]W. Shockley, Solid State Technol **26**(1), 76–78 (1983).